AJNR

Occult Amyloid-β-Related Angiitis: Neuroimaging Findings at 1.5T, 3T, and 7T MRI

Can Özütemiz, Haitham M. Hussein, Salman Ikramuddin, H. Brent Clark, Andreas Charidimou and Christopher Streib

Occult Amyloid-β-Related Angiitis: Neuroimaging Findings at 1.5T, 3T, and 7T MRI

Can Özütemiz, Haitham M. Hussein, Salman Ikramuddin, H. Brent Clark, Andreas Charidimou, and ⬤Christopher Streib

ABSTRACT

SUMMARY: Cerebral amyloid angiopathy (CAA) is a progressive neurodegenerative small vessel disease that is associated with intracranial hemorrhage and cognitive impairment in the elderly. The clinical and radiographic presentations have many overlapping features with vascular cognitive impairment, hemorrhagic stroke, and Alzheimer disease (AD). Amyloid-β-related angiitis (ABRA) is a form of primary CNS vasculitis linked to CAA, with the development of spontaneous autoimmune inflammation against amyloid in the vessel wall with resultant vasculitis. The diagnosis of ABRA and CAA is important. ABRA is often fatal if untreated and requires prompt immunosuppression. Important medical therapies such as anticoagulation and antiamyloid agents for AD are contraindicated in CAA. Here, we present a biopsy-proved case of ABRA with underlying occult CAA. Initial 1.5T and 3T MR imaging did not suggest CAA per the Boston Criteria 2.0. ABRA was not included in the differential diagnosis due to the lack of any CAA-related findings on conventional MR imaging. However, a follow-up 7T MR imaging revealed extensive cortical/subcortical cerebral microbleeds, cortical superficial siderosis, and intragyral hemorrhage in extensive detail throughout the supratentorial brain regions, which radiologically supported the diagnosis of ABRA in the setting of CAA. This case suggests an increased utility of high-field MR imaging to detect occult hemorrhagic neuroimaging findings with the potential to both diagnose more patients with CAA and diagnose them earlier.

ABBREVIATIONS: ABRA = amyloid-β-related angiitis; AD = Alzheimer disease; CAA = cerebral amyloid angiopathy; CSS = cortical superficial siderosis; PCR = polymerase chain reaction; PiB-PET = Pittsburgh compound-B; SPACE = sampling perfection with application-optimized contrasts by using different flip angle evolution; GRE = gradient-echo

An 84-year-old woman presented to the emergency department with 1 week of right temporal headache, nausea, vomiting, unsteady gait, and visual hallucinations. Her blood pressure at presentation was 163/73 mm Hg. The neurologic examination was notable for mild encephalopathy and intermittent visual hallucinations, which she was aware were not real. A head CT scan was unremarkable apart from age-related mild generalized cerebral volume loss. Notably, the patient and her husband reported the same symptoms 10 years ago. Review of her previous work-up was notable for a brain MR imaging with multiple areas of restricted diffusion and leptomeningeal enhancement. Additionally, her CSF at the time demonstrated elevated leukocytes (137/μL) without evidence of infection. She was presumptively diagnosed with CNS vasculitis and had complete resolution of symptoms after empiric treatment with corticosteroids. The patient remained symptom-free for 10 years.

Conventional MR Imaging Findings at 1.5T and 3T

The patient was admitted for further evaluation. A contrast-enhanced 1.5T MR imaging performed the next day showed multiple bilateral small cortical foci of restricted diffusion and bilateral scattered areas of leptomeningeal enhancement in the supratentorial brain, not corresponding to a specific vascular territory (Fig 1). The distribution of these findings was similar to her previous MR imaging. The T2* gradient-echo (T2*-GRE) sequence was unremarkable without any evidence of intracranial hemorrhage, cerebral microbleeds, or cortical superficial siderosis (CSS) (Fig 1). FLAIR showed nonspecific periventricular white matter hyperintensities, with sparing of subcortical regions, consistent with chronic small vessel ischemic disease. MR and CT angiography showed no evidence of vascular occlusion, stenosis, nonstenotic soft plaque, or vasculitic changes, and the atherosclerotic burden in the aorta and large vessels was minimal.

Due to a history of prior CNS vasculitis diagnosis, a limited black-blood vessel wall imaging was subsequently obtained at 3T by using a 3D-T1-sampling perfection with application-optimized contrasts by using different flip angle evolution
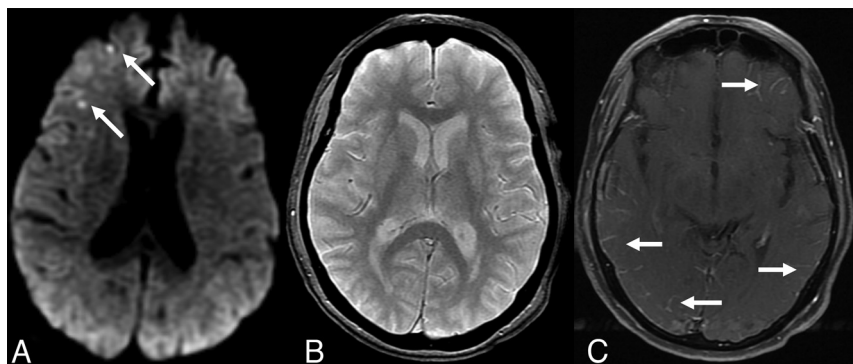
FIG 1. MR imaging at 1.5T obtained in the emergency department. Axial DWI (*A*), T2*-GRE (*B*), and contrast-enhanced T1-TSE (*C*) images at identical section levels. *A*, *Arrows* show punctuate areas of restricted diffusion in the right frontal cortex. There were a few more similar foci in other regions of the brain (not shown). *B*, T2*-GRE was negative for any intracranial hemorrhage or cerebral microbleeds. *C*, *Arrows* point to bilateral multifocal abnormal leptomeningeal enhancement.
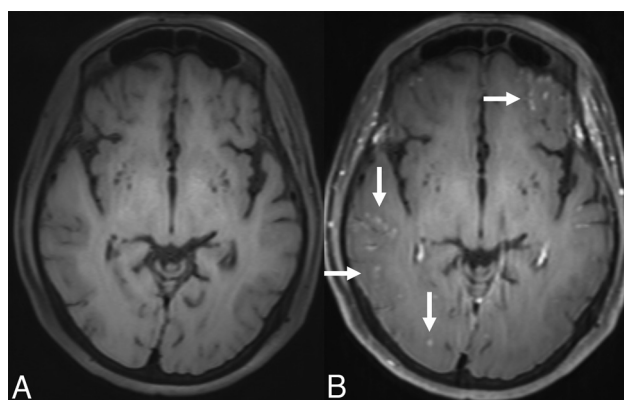

FIG 2. Axial precontrast (*A*) and axial postcontrast (*B*) black-blood vessel wall MR imaging obtained at 3T. Correlated with precontrast vessel wall MR imaging (*A*), postcontrast image (*B*) shows bilateral scattered leptomeningeal disease (*arrows*) in the supratentorial regions. No definite periarterial or arterial wall enhancement is appreciated.

(SPACE) sequence, with and without contrast agent, on a separate day. This study did not show any perivascular enhancement or arterial stenosis to suggest arterial vasculitis in the large and middle-sized intracranial arteries. Still, scattered leptomeningeal enhancement was again noted (Fig 2).

Diagnostic Evaluation
An extensive evaluation for conventional stroke etiologies was completed, which included low-density lipoprotein (99 mg/dL) and hemoglobin A_{1c} (6.2%, in the prediabetic range). Electrocardiogram showed normal sinus rhythm, and telemetry did not reveal any arrhythmia. Echocardiography demonstrated an ejection fraction of 60%–65%, biatrial enlargement, and severe mitral annular calcification without cardioembolic source of stroke. Similarly, cardiac CTA did not show evidence of intracardiac thrombus or aortic arch atheroma. CT of the chest/abdomen/pelvis did not show underlying malignancy that might cause a hypercoagulable state or a source of infection. Blood pressure was well-controlled throughout the patient's admission after a period of permissive hypertension (systolic blood pressure range: 129–163).

Due to high suspicion for an atypical cause of stroke, a more extensive diagnostic work-up was pursued. A lumbar puncture showed increased leukocytes (24/Ul), erythrocytes (360/Ul), and protein (109 mg/Dl). Additional CSF studies included an elevated IgG index, no oligoclonal bands, normal angiotensin-converting enzyme, negative meningitis/encephalitis panel (including herpes simplex virus 1 and 2 and varicella zoster virus), and negative flow cytometry. Other laboratory tests that were negative or in the normal range included troponin, brain natriuretic peptide, thyroid-stimulating hormone, erythrocyte sedimentation rate, C-reactive protein, antinuclear antibody, double-stranded DNA, antineutrophilic cytoplastic antibody, rheumatoid factor, anticardiolipin, lupus anticoagulant, β-2-glycoprotein, QuantiFERON gold, Lyme serology, and coronavirus disease 2019 (COVID-19) polymerase chain reaction (PCR) testing.

Pathology
Based on the aforementioned findings and past medical history, the neurology team suspected that the patient could have acute CNS vasculitis. However, her clinical course with no residual symptoms or recurrence in 10 years was atypical. The differential diagnosis also included occult malignancy, such as intravascular lymphoma, a neuroinflammatory process, infectious endocarditis, or atypical presentation of embolic stroke from atherosclerosis or cardioembolism. Due to the persistent diagnostic uncertainty, a brain biopsy was obtained to confirm the diagnosis before committing to long-term immunosuppression. A biopsy was obtained from the right frontal dura mater and underlying parenchyma in an area with leptomeningeal enhancement.

On pathologic examination, the sections of dura mater were unremarkable, with no evidence of vascular pathology. Sections from the brain had extensive granulomatous vasculitis, particularly involving leptomeningeal arteries. The arterial walls were infiltrated by epithelioid histiocytes and lymphocytes to a lesser extent. Most of the affected vessel walls, where visible, had amyloid deposition, confirmed by Aβ immunohistochemistry. In some of the granulomas, no vascular profile was seen, and some had little or no Aβ staining, possibly because the vascular wall was not within the thickness of the section and only the granulomatous element was present. There was a recent microinfarct in one area with vacuolation of the white matter and numerous axonal spheroids, which stained heavily with Aβ antibodies. In addition, there were numerous plaquelike accumulations of Aβ in the cerebral cortex, which were not well-appreciated on the H&E-stained sections, suggestive of the early "diffuse" type of senile plaque formation (Fig 3).

Overall, the histopathologic findings supported a diagnosis of amyloid-β-related angiitis (ABRA), a form of primary CNS vasculitis linked to cerebral amyloid angiopathy (CAA). There appeared to be vascular mural injury in some of the affected
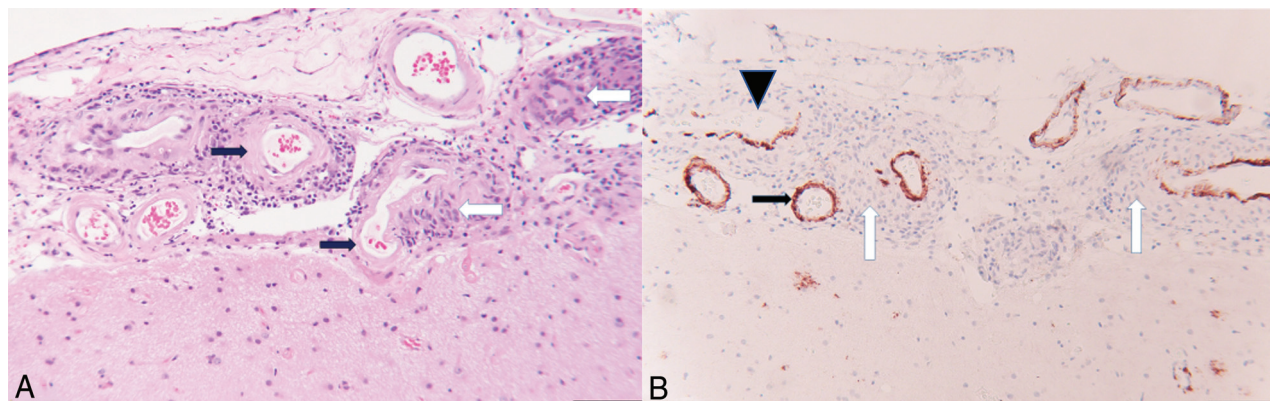
FIG 3. A, H&E-stained section from the right frontal lobe biopsy with granulomatous angiitis (*white arrows*) in the leptomeninges. The affected vessels have hyalinization of the tunica media and loss of smooth muscle nuclei, consistent with amyloid angiopathy (*black arrows*). B, Immunohistochemical staining for amyloid-β counterstained with hematoxylin. The leptomeningeal vessels involved by granulomatous inflammation (*white arrows*) have brown immunoreactivity for amyloid-β (*black arrow*). The vessel in the upper left has partial destruction of the wall with focal loss of amyloid immunoreactivity (*black arrowhead*). Scale bar =100 μm at (A) and (B).
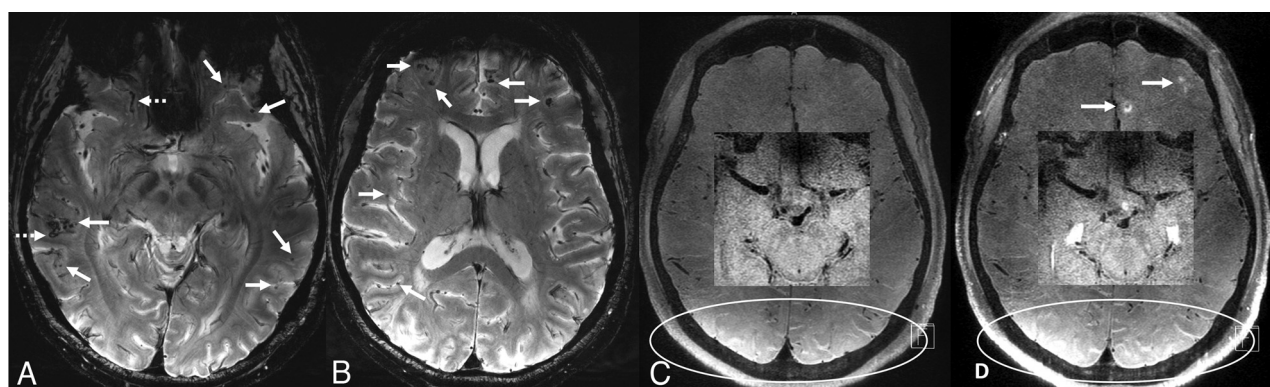

FIG 4. 7T brain MR imaging obtained after discharge. Axial T2* images (*A and B*) show numerous scattered punctate susceptibility artifacts in the cortical/subcortical distribution (*solid arrows*), consistent with cerebral microbleeds and cortical superficial siderosis in the supratentorial parenchyma (*dashed arrows*), which are completely obscured at 1.5T GRE (Fig 1). Precontrast (*C*) and postcontrast (*D*) black blood vessel wall MR imaging with zoomed smaller images at the center, focusing on larger vessels at the circle of Willis. Compared with vessel wall MR imaging at 3T (Fig 2), the vessel walls have higher resolution and improved appearance. *Arrows* at (*D*) show leptomeningeal enhancement in the left frontal regions, which is harder to appreciate compared with 3T. Note that it is harder to suppress the peripheral CSF signal (*white oval windows*) at 7T, leptomeningeal enhancement at these regions cannot be perceived without a precontrast control study, or these regions could be equivocally called enhancement. No suspicious stenosis, contrast enhancement, or wall thickening is identified at the circle of Willis.

arteries and not just perivascular inflammation, the latter of which sometimes occurs as a more benign inflammatory reaction associated with cerebrovascular amyloid deposits.

Postoperative Clinical Follow-up and Radiologic Follow-up at 7T MR Imaging

The patient was treated with 3 days of pulse-dose steroids (1000 mg methylprednisolone daily) before the brain biopsy results were available. Clinically, a marked improvement was observed with resolution of headache and visual hallucinations, along with improved cognitive function and gait. The patient was discharged home with a prescription for aspirin 325 mg/d.

While the biopsy results were still pending, to continue the patient's diagnostic work-up, the patient underwent 7T MR imaging/MRA 1 week later with an FDA-approved Magnetom Terra MR imaging scanner (Siemens) equipped with 1-channel transmit/32-channel receive array head coil (Nova Medical) by using

the first level mode. During image acquisition, in-house calcium titanate dielectric pads were placed in the temporal and suboccipital regions. Apart from conventional sequences, this 7T MR imaging examination also included black-blood vessel wall imaging (sagittal 3D fat-saturated T1-weighted SPACE; TR/TE: 1100/23 ms, section thickness: 0.5 mm, matrix: 272 × 272, FOV: 136 mm, voxel size: 0.3 × 0.3 × 0.5 mm^3; acquisition time: 5:06 min). DWI at 7T showed new punctate lesions with diffusion restriction. Axial T2* sequence showed extensive CSS with numerous punctate cortical and subcortical cerebral microbleeds consistent with CAA, which were not visualized on prior MRIs with lower magnetic field strength (Fig 4). Vessel wall MR imaging showed markedly superior resolution of the vessel walls of the large and medium-sized arteries compared with 3T, without any suspicious vessel wall enhancement. Subtle leptomeningeal enhancement in the left inferior frontal regions was perceived after careful correlation of pre- and postcontrast series and with
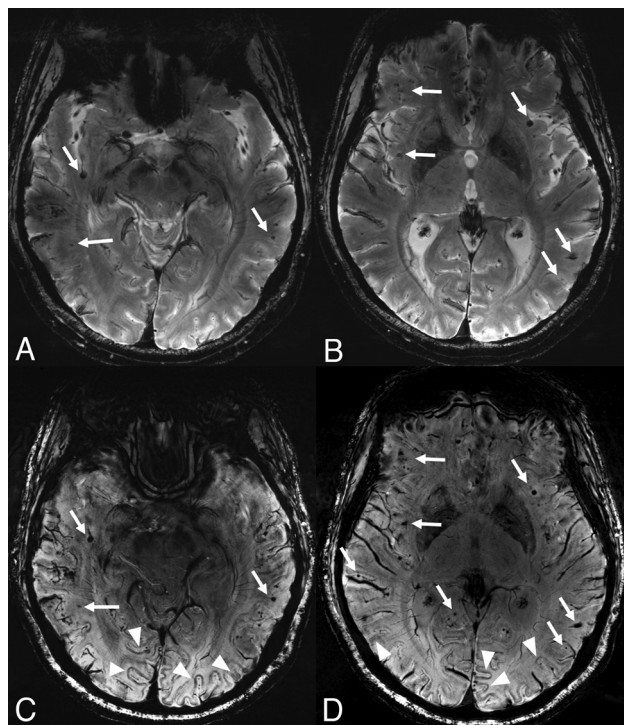
FIG 5. Three-month follow-up 7T MR imaging. Axial T2* images are at the upper row (*A and B*) and corresponding axial SWI (*C and D*) are at the lower row. After 3 months, the patient is symptom-free, however, images show an increased number of punctate microhemorrhages in comparison with the corresponding images at previous 7T MR imaging axial T2* (Fig 4*A, -B*). *Arrows* point out some of the peripheral microhemorrhages and compared with T2* (*A and B*), SWI provides a clearer and sharper visualization of some of these microhemorrhages (*C and D*). In closer look, the entire cortex shows a gyriform susceptibility artifact in certain regions on SWI, most significant in the occipital lobes, which is not technically a superficial pial siderosis but actually corresponds to newly described intragyral hemorrhage sign (*arrowheads* in *C and D*). This observation was not well appreciated on T2*.

retrospective review of the older 3T MR imaging, which was obtained before treatment with steroids. Assessment of other superficial areas on vessel wall MR imaging at 7T, including occipital and parietal gyri, was obscured due to high peripheral CSF T1 signal in contrast to low T1 CSF signal seen in the central portions of the brain (Fig 4). Altogether, the radiographic findings on high-field MR imaging were also consistent with ABRA.

After the radiographic and histopathologic diagnosis of ABRA secondary to CAA, aspirin monotherapy was continued for secondary stroke prevention in the setting of the patient's recurrent ischemic strokes. Due to her excellent recovery, the patient had already been discharged home, and she elected not to pursue additional oral steroid treatment with close radiographic and clinical surveillance. Her neurologic examination at her 3-month follow-up visit showed only mild amnestic cognitive impairment, which was her baseline. A repeat 7T MR imaging was obtained for surveillance. This scan was optimally protocolized for evaluation of CAA including both ultra-high resolution axial SWI (TR/TE: 22/15 ms, section thickness: 1.4 mm, matrix: 640 × 640, FOV: 220 mm, voxel size: 0.2 × 0.2 × 1.4 mm^3; acquisition time: 6:30 min) and axial T2* (TR/TE: 1080/20 ms, section thickness:

1.5 mm, matrix: 620 × 620, FOV: 210 mm, voxel size: 0.2 × 0.2 × 1.5 mm^3; acquisition time: 9:35 min). Both sequences showed further increased number of microbleeds in the cortical-subcortical regions and new areas of CSS in a wider distribution compared with axial T2* obtained 3 months earlier (Fig 5). While all microbleeds were visible on both SWI and T2*, the lesions were easier to observe and appeared clearer and sharper on SWI. Only seen on the SWI sequence, there were several areas in the occipital lobes with susceptibility artifacts involving the entire cortical ribbon, in a tram-track fashion. This finding was not well appreciated on T2*. This tram-tracklike dark appearance of the gyri in the occipital lobes was not an MR imaging finding we were accustomed to seeing on 3T MR imaging in other CAA cases. There were also 4 new areas of punctate DWI restriction, 1 correlated with a microbleed, while the other 3 appeared to be secondary to subacute infarctions. The postcontrast 3D T1-MPRAGE was negative for any leptomeningeal enhancement. Despite the increased microhemorrhage and new punctate areas of restricted diffusion, the patient's clinical improvement was remarkable. Given her clinical stability and the resolution of leptomeningeal enhancement, the patient and her vascular neurologist elected not to initiate further immunotherapy. The patient was maintained on aspirin monotherapy with close follow-up and has continued to recover well.

DISCUSSION

CAA is a progressive neurodegenerative small vessel disease that is associated with intracranial hemorrhage and cognitive impairment in the elderly. The pathophysiologic mechanism is abnormal accumulation of primarily Aβ-40 peptide fragments in the walls of cortical and leptomeningeal small arteries, arterioles, and capillaries.[1-4] The disease has overlapping features with Alzheimer disease (AD), in which Aβ-42 peptide fragments accumulate in the brain parenchyma.[3,5] While the diagnosis can only be confirmed with biopsy and histopathologic examination, in usual clinical practice, the diagnosis is based on key clinical features and MR imaging findings in the context of Boston Criteria Version 2.0 (Online Supplemental Data).[1] The clinical and radiographic presentations have many overlapping features with vascular dementia, stroke, and AD. Thus, accurate recognition of CAA is imperative, because the treatments for these entities are markedly different. In particular, CAA is a contraindication to certain standard-of-care medications, including anticoagulation for stroke or immunotherapies against AD.[6,7] Withholding essential anticoagulation or antiamyloid therapies requires a high degree of confidence in the CAA diagnosis.

ABRA occurs in CAA with the development of spontaneous autoimmune inflammation against the amyloid in the vessel wall and resultant vasculitis.[2,8] This entity represents a spontaneous human example of amyloid-related imaging abnormalities, an autoimmune reaction following immune therapy in AD.[3] Early recognition of ABRA is essential because it can be progressive and fatal, but often responds to prompt treatment based on immune suppression and high-dose steroid treatment.[2]

Here, we present an atypical case of ABRA with underlying occult CAA. Initial MR images did not suggest CAA per the Boston Criteria 2.0 on conventional 1.5 and 3T MR images.

Although vasculitis was strongly suspected based on the patient's reported medical history and the MR imaging findings demonstrating multiple bilateral infarcts of various ages and leptomeningeal enhancement, ABRA had not been included in the differential diagnosis due to the lack of any CAA-related findings and lack of edema in the cortex or subcortical white matter on FLAIR, hence not fulfilling the criteria for probable CAA-related inflammation (Online Supplemental Data). A limitation of this case is that SWI was not obtained on the initial 1.5T and 3T MRIs. Although SWI should be the clinical standard over T2*-GRE because SWI has higher sensitivity than T2*-GRE for CSS and microhemorrhage detection, not all hospitals have switched from T2*-GRE to SWI for many local reasons. For example, T2*-GRE requires less acquisition time and is less prone to motion artifact; therefore, it is still favored by many experienced neuroradiologists. Given the marked disparity between findings at 1.5T and 3T versus 7T, it is unlikely that incorporating SWI alone would have revealed the degree of underlying radiographic markers of CAA that we observed on 7T imaging. This is consistent with the previously reported utility of 7T MR imaging in CAA, including demonstration of novel imaging findings such as intragyral hemorrhage and "striped occipital cortex" sign.[9] Regardless, this case also highlights the importance of using SWI over less sensitive sequences in patients with cerebrovascular disease.

It is known that there is significantly increased sensitivity to magnetic susceptibility artifacts, signal-to-noise ratio, and contrast-to-noise ratio in ultra-high field 7T MR imaging in comparison to 1.5T and 3T MR imaging. The scientific literature on CAA and ABRA, including the Boston Criteria 2.0 is predominantly based on GRE and SWI sequences obtained on 1.5 and 3T MR imaging scanners. The Boston Criteria 2.0 (nor its previous iterations) are not validated for 7T MR imaging.[9] Nonetheless, it remains intuitive that 7T MR imaging would have increased sensitivity for microbleeds and CSS, leading to more frequent and earlier diagnoses of CAA. Two 7T MR imaging postmortem studies in patients with CAA by using a T2* sequence showed novel diffuse susceptibility artifact involving the entire portion of the cortical ribbon, referred to as intragyral hemorrhage.[10,11] Moreover, a novel "striped occipital cortex" sign in CAA was also described at 7T.[11]

Histopathology samples corresponding to the "striped occipital cortex" demonstrated iron depositions and calcification of the penetrating arteries of the cerebral occipital cortex.[12] Koemans et al[11] assessed the presence of these novel MR imaging findings in patients with hereditary cerebral hemorrhage with amyloidosis by using 7T MR imaging. They reported the intragyral hemorrhage sign and the striped occipital cortex sign in 12% and 3% of the patients, respectively, while these signs were absent in control subjects.[11] Similar to our case, they reported that these MR imaging findings could not be observed at conventional MR imaging magnet strength. While subtle cortical microhemorrhages seen on 7T could be related to other conditions such as microinfarcts or AD,[13,14] in the appropriate clinical context, the distribution of microhemorrhages and presence of CSS, intragyral hemorrhage, or striped occipital cortex signs should reliably suggest a CAA diagnosis.

Amyloid PET imaging has been explored as a potential molecular biomarker for CAA. However, its utility for CAA diagnosis remains limited due to the inability of current radioligands to distinguish between vascular and parenchymal amyloid deposits. Increased signal on an amyloid PET might be due to parenchymal amyloid, vascular amyloid, or a combination of the two, depending on the clinical context.[15] A recent neuropathologic study by using antemortem PET scans with Pittsburgh compound-B (PiB-PET) found no correlation between PiB-PET signal and histopathologic CAA burden on a gross lobar level.[16] In practice, this means that CAA alone might not be enough to lead to a positive amyloid PET scan, at least in patients presenting with memory complaints without major hemorrhagic stroke. Another study by using the amyloid PET tracer ^{18}F-florbetapir found that patients with CAA had a lower global amyloid PET uptake compared with patients with mild cognitive impairment due to AD.[17] Although not statistically significant, this study noted relatively increased ^{18}F-florbetapir uptake in the posterior brain regions of patients with CAA, aligning with prior findings that CAA preferentially affects posterior areas of the brain.[18] Of note, how the active autoinflammatory reaction against vascular amyloid, as observed in ABRA, affects the amyloid PET uptake remains uncertain. For these and other reasons, brain MR imaging remains the preferred diagnostic approach for CAA. Advances in MR imaging technology, particularly the use of 7T MR imaging, hold promise for enhancing the diagnostic sensitivity and specificity for CAA.

FDA-approved 7T MR imaging scanners are available in only a few centers in the United States. Sequence parameters and protocols are not fully optimized, and there are only a few resources to guide neuroradiologists in this unknown territory.[19,20] T2* and SWI are the 2 primary sequences sensitive to microbleeds and CSS. In this single case, SWI provided a better delineation of the microbleeds and intragyral hemorrhage, though the difference was minor, and both sequences could detect these abnormalities. SWI may be preferable to T2* due to the shorter acquisition time, but differences in these sequences on 7T should be studied in larger cohorts in the future.

Another consideration is that 7T vessel wall MR imaging may better delineate the walls of large and middle-sized arteries and aneurysms compared with 3T.[21,22] However, peripheral leptomeningeal enhancement can be missed due to incomplete CSF suppression in the periphery with 3D T1-SPACE sequences in contrast to the image center. Vessel wall MR imaging showed either leptomeningeal enhancement or vessel wall enhancement in the peripheral small vessels in CAA cohorts.[23,24] Therefore, neuroradiologists should be familiar with this issue, and perhaps 3D-T1-MPRAGE sequence might be preferred for assessing leptomeningeal disease in the setting of vasculitis or ABRA at 7T.

This case is the only reported biopsy-proved ABRA case in CAA, which has prior imaging with 1.5T, 3T, and 7T MR imaging and contrast-enhanced vessel wall MR imaging, allowing us to compare vessel wall MR imaging findings between 3T and 7T, as well as to illustrate a dramatic comparison of GRE at 1.5T with SWI and T2* at 7T, and a direct comparison of SWI and T2* at 7T. This case suggests an increased utility of high-field MR imaging to detect occult hemorrhagic neuroimaging findings with the potential to both diagnose more patients with CAA and diagnose them earlier. Additionally, larger research studies are imperative.

Case Summary

CAA may mimic other neurologic diseases clinically and radiologically. In this case, the diagnosis of ABRA, an autoimmune vasculitis that occurs in the setting of CAA, was delayed due to the inability to visualize neuroimaging markers of CAA on conventional MR imaging. However, 7T MR imaging demonstrated typical cortical and subcortical microbleeds with CSS. A 7T MR imaging also revealed intragyral hemorrhage sign, a recently described finding in CAA on high-field MR imaging. The diagnosis of ABRA and CAA are important: ABRA is often fatal if untreated, whereas CAA is a contraindication to standard-of-care medications such as anticoagulation to prevent stroke and antiamyloid agents for cognitive impairment. Finally, the increased sensitivity for CAA and ABRA on 7T MR imaging could potentially reduce the need for brain biopsy.

Disclosure forms provided by the authors are available with the full text and PDF of this article at www.ajnr.org.

REFERENCES

1. Charidimou A, Boulouis G, Frosch MP, et al. **The Boston criteria version 2.0 for cerebral amyloid angiopathy: a multicentre, retrospective, MRI-neuropathology diagnostic accuracy study.** *Lancet Neurol* 2022;21:714–25 CrossRef Medline

2. Bangad A, Abbasi M, Payabvash S, et al. **Imaging of amyloid-beta-related arteritis.** *Neuroimaging Clin N Am* 2024;34:167–73 CrossRef Medline

3. Agarwal A, Gupta V, Brahmbhatt P, et al. **Amyloid-related imaging abnormalities in Alzheimer disease treated with anti-amyloid-beta therapy.** *Radiographics* 2023;43:e230009 CrossRef Medline

4. Mandybur TI. **Cerebral amyloid angiopathy: the vascular pathology and complications.** *J Neuropathol Exp Neurol* 1986;45:79–90 CrossRef Medline

5. Ghiso J, Tomidokoro Y, Revesz T, et al. **Cerebral amyloid angiopathy and Alzheimer's disease.** *Hirosaki Igaku* 2010;61:S111–24 CrossRef Medline

6. Roytman M, Mashriqi F, Al-Tawil K, et al. **Amyloid-related imaging abnormalities: an update.** *AJR Am J Roentgenol* 2023;220:562–74 CrossRef Medline

7. Ozutemiz C. **Editorial comment: novel immunotherapies for Alzheimer disease and cerebral amyloid angiopathy create new challenges and opportunities in neuroimaging.** *AJR Am J Roentgenol* 2023;220:575 CrossRef

8. Amin M, Aboseif A, Southard K, et al. **The prevalence of radiological cerebral amyloid angiopathy-related inflammation in patients with cerebral amyloid angiopathy.** *J Stroke Cerebrovasc Dis* 2023;32:107436 CrossRef Medline

9. Koemans EA, Voigt S, Rasing I, et al. **Striped occipital cortex and intragyral hemorrhage: novel magnetic resonance imaging markers for cerebral amyloid angiopathy.** *Int J Stroke* 2021;16:1031–38 CrossRef Medline

10. De Reuck J, Deramecourt V, Cordonnier C, et al. **Superficial siderosis of the central nervous system: a post-mortem 7.0-Tesla magnetic resonance imaging study with neuropathological correlates.** *Cerebrovasc Dis* 2013;36:412–17 CrossRef Medline

11. Koemans EA, van Etten ES, van Opstal AM, et al. **Innovative magnetic resonance imaging markers of hereditary cerebral amyloid angiopathy at 7 Tesla.** *Stroke* 2018;49:1518–20 CrossRef Medline

12. Bulk M, Moursel LG, van der Graaf LM, et al. **Cerebral amyloid angiopathy with vascular iron accumulation and calcification.** *Stroke* 2018;49:2081–87 CrossRef Medline

13. De Reuck J, Auger F, Durieux N, et al. **Topography of cortical microbleeds in Alzheimer's disease with and without cerebral amyloid angiopathy: a post-mortem 7.0-Tesla MRI study.** *Aging Dis* 2015;6:437–43 CrossRef Medline

14. Lakhani DA, Zhou X, Tao S, et al. **7T MRI in transient ischemic attacks: have we only seen the tip of the iceberg?** *Neuroradiol J* 2023 Mar 27. [Epub ahead of print] CrossRef Medline

15. Farid K, Charidimou A, Baron JC. **Amyloid positron emission tomography in sporadic cerebral amyloid angiopathy: a systematic critical update.** *Neuroimage Clin* 2017;15:247–63 CrossRef Medline

16. McCarter SJ, Lesnick TG, Lowe V, et al. **Cerebral amyloid angiopathy pathology and its association with amyloid-beta PET signal.** *Neurology* 2021;97:e1799–e1808 CrossRef Medline

17. Planton M, Saint-Aubert L, Raposo N, et al. **Florbetapir regional distribution in cerebral amyloid angiopathy and Alzheimer's disease: a PET study.** *J Alzheimers Dis* 2020;73:1607–14 CrossRef Medline

18. Reijmer YD, Fotiadis P, Riley GA, et al. **Progression of brain network alterations in cerebral amyloid angiopathy.** *Stroke* 2016; 47:2470–75 CrossRef Medline

19. Ozutemiz C, White M, Elvendahl W, et al. **Use of a commercial 7-T MRI scanner for clinical brain imaging: indications, protocols, challenges, and solutions-a single-center experience.** *AJR Am J Roentgenol* 2023;221:788–804 CrossRef Medline

20. Opheim G, van der Kolk A, Markenroth Bloch K, et al. **7T epilepsy task force consensus recommendations on the use of 7T MRI in clinical practice.** *Neurology* 2021;96:327–41 CrossRef Medline

21. Feng J, Liu X, Zhang Z, et al. **Comparison of 7 T and 3 T vessel wall MRI for the evaluation of intracranial aneurysm wall.** *Eur Radiology* 2022;32:2384–92 CrossRef Medline

22. Harteveld AA, van der Kolk AG, van der Worp HB, et al. **High-resolution intracranial vessel wall MRI in an elderly asymptomatic population: comparison of 3T and 7T.** *Eur Radiology* 2017;27:1585–95 CrossRef Medline

23. Hao Q, Tsankova NM, Shoirah H, et al. **Vessel wall MRI enhancement in noninflammatory cerebral amyloid angiopathy.** *AJNR Am J Neuroradiol* 2020;41:446–48 CrossRef Medline

24. McNally JS, Sakata A, Alexander MD, et al. **Vessel wall enhancement on black-blood MRI predicts acute and future stroke in cerebral amyloid angiopathy.** *AJNR Am J Neuroradiol* 2021;42:1038–45 CrossRef Medline